M07

Proceedings of the 5th International Conference on Inverse Problems in Engineering: Theory and Practice, Cambridge, UK, 11-15th July 2005

SOME INVERSE PROBLEMS IN SYSTEMS OF NONLINEAR PARABOLIC EQUATIONS

D. A. MURIO
Department of Mathematical Sciences, University of Cincinnati, Cincinnati, OH 45221-0025, USA
email: diego@dmurio.csm.uc.edu

Abstract - Assuming only Cauchy noisy data at the active boundary, we investigate the inverse problem of numerically recovering the solutions, gradient distributions and initial conditions, in nonlinear systems of parabolic partial differential equations with space dependent coefficients, by means of stable space marching methods. If the initial condition of the system is known, we also discuss, in the Cauchy data case, the inverse problems associated with the identification of some of the space dependent coefficients in the Lotka-Volterra model with diffusion, while marching in space. Stability and error analysis of the algorithms, together with numerical results of interest, are presented.

1. INTRODUCTION

A stable numerical marching scheme based on discrete mollification is used to recover the solution vector $u(x,t)$, including $u(x,0)$, in a nonlinear parabolic system of the form

$$\begin{aligned} &u_t = (a(x)u_x)_x + f(u,x), \\ &0 < x < x_1,\ 0 < t < t_1, \\ &u(0,t) = 0, \\ &u_x(0,t) = \alpha(t), \\ &0 \le t \le t_1, \end{aligned}$$

with positive constants x_1 and t_1.

Note that in this problem, the data vector $\alpha(t)$ is known approximately and the space dependent diffusion, $a(x)$, and the interaction function, $f(u,x)$, are known throughout the rectangular domain. The proposed algorithm does not require a priori information about the noise in the data and the mollification parameters are chosen automatically at each step using the Generalized Cross Validation (GCV) method, [6]. For a detailed description of mollification techniques, the reader is referred to [2].

In a related problem, if the initial condition $u(x,0)$ is given, we study the approximate identification of some of the space dependent coefficients in the Lotka-Volterra model with diffusion. For instance, given F interactive species, the source elements are given by

$$f_i(u,x) = u_i(b_i(x) + \sum_{j=1}^{F} B_{ij}(x)u_j),\ i = 1,\dots,F,$$

and it is possible to recover F unknown coefficients from the set of $F(1+F)$ components of the F dimensional vector b and the $F \times F$ dimensional matrix B.

This article is organized as follows: in section 2, we state basic properties and estimates corresponding to mollification. In section 3, the numerical marching scheme is introduced. The proof of stability and convergence is given in section 4. Two numerical examples of interest are shown in section 5. The second one illustrates the general procedure for the identification of space dependent coefficients in some specific biological models.

2. DISCRETE MOLLIFICATION

Let $g : I = [0,1] \to \mathbb{R}$ and $G = \{g_i\}_{i=1}^{M}$ be the discrete version of g defined on the set $K = \{y_i : i \in \mathbb{Z}, 1 \le i \le M\}$, $0 \le y_1 \le \cdots \le y_M \le 1$. The discrete δ - mollification of G is the convolution with the Gaussian kernel

$$\rho_\delta(y) = \begin{cases} A_\rho \delta^{-1} \exp\left(-\dfrac{y^2}{\delta^2}\right), & y \in I_\delta, \\ 0, & y \notin I_\delta, \end{cases}$$

where $I_\delta = [-p\delta, p\delta]$, $p > 0$, $\delta > 0$ and $A_p = \left(\int_{-p}^{p} \exp(-s^2) ds \right)^{-1}$.

That is, for every $y \in I_\delta$,

$$J_\delta G(y) = \sum_{i=1}^{M} g_i \int_{s_{i-1}}^{s_i} \rho_\delta (y - s) ds,$$

where $s_0 = 0, s_M = 1$, and $s_i = \frac{y_{i+1} + y_i}{2}, i = 1, 2, ..., M-1$.

The radius of mollification δ, is chosen automatically using the GCV method.

The perturbed version of G is given by $G^\varepsilon = \{g_i^\varepsilon = g_i + \varepsilon_i : | \varepsilon_i | \le \varepsilon, i = 1, 2, ..., M\}$, where the ε_i's are a family of independent random variables, uniformly distributed in the interval $[-\varepsilon, \varepsilon]$, and ε represents the maximum level of noise in the data. That is, if $\| . \|_\infty$ denotes the maximum norm, then $\| G - G^\varepsilon \|_{\infty,K} \le \varepsilon$.

First and second derivatives are approximated, respectively, using the finite difference operators

$$D_0(g(x)) = [g(x + \Delta x) - g(x - \Delta x)]/(2\Delta x)$$

and

$$D_0^2(g(x)) = [g(x + \Delta x) + 2g(x) - g(x - \Delta x)]/(\Delta x)^2$$

on the interval $\tilde{I}_\delta = [p\delta + \Delta x, 1 - p\delta - \Delta x]$.

The following lemma establishes the numerical properties of discrete mollified differentiation, as defined above, for fixed δ. Note that, throughout the paper, C denotes a generic constant that is independent of δ.

Lemma 2.1 (Stability and Convergence) *If* $g \in C^2(I)$, $g^\varepsilon \in C^0(I)$, *and* $\| G - G^\varepsilon \|_{\infty,I} \le \varepsilon$, *then there exist constants* C *and* C_δ, *such that*

$$\| g - J_\delta G^\varepsilon \|_{\infty, I_\delta} \le C(\delta + \varepsilon + \Delta x),$$

$$\left\| D_0(J_\delta G^\varepsilon) - \frac{\partial g}{\partial x} \right\|_{\infty, I_\delta} \le C\left(\frac{\varepsilon + \Delta x}{\delta}\right) + C_\delta (\Delta x)^2,$$

and

$$\left\| D_0^2(J_\delta G^\varepsilon) - \frac{\partial^2 g}{\partial x^2} \right\|_{\infty, I_\delta} \le C\left(\frac{\varepsilon + \Delta x}{\delta^2}\right) + C_\delta (\Delta x)^2.$$

The proof of Lemma 2.1 can be found in [3].

We define $D_0^\delta(J_\delta G) = D_0(J_\delta G)|_{\tilde{I}_\delta \cap K}$, by restricting $D_0(J_\delta G)$ to the grid points of $\tilde{I}_\delta \cap K$.

The next theorem provides an upper bound for the maximum norm of the operator D_0^δ.

Theorem 2.2 *There exists a constant* C *such that*

$$\| D_0^\delta G \|_{\infty, \tilde{I}_\delta \cap K} \le \frac{C}{\delta} \| G \|_{\infty, K} .$$

The proof of this theorem can also be found in [3].

3. MARCHING SCHEME

The regularized problem is obtained by mollifying the original system. The numerical marching scheme attempts to compute a meaningful approximation to the solution, the initial condition, and gradient distribution vectors,

$$v(x,t) = (v_1(x,t), \ldots, v_F(x,t))^T,$$
$$v(x,0) = (v_1(x,0), \ldots, v_F(x,0))^T,$$
$$v_x(x,t) = ((v_1)_x(x,t), \cdots, (v_F)_x(x,t))^T$$

and

$$v_t(x,t) = ((v_1)_t(x,t), \cdots (v_F)_t(x,t))^T,$$

of the mollified system of parabolic partial differential equations given by

$$
\begin{aligned}
&v_t = (a(x)v_x)_x + f(v,x),\\
&0 < x < x_1,\ 0 < t < t_1,\\
&v(0,t) = 0,\\
&v_x(0,t) = J_\delta \alpha^\varepsilon(t),\\
&0 \le t \le t_1.
\end{aligned}
$$

The available data function $\alpha^\varepsilon(t)$ is a discrete vector function such that $\|\alpha^\varepsilon - \alpha\|_{\infty,K} \le \varepsilon$ and it has been mollified.

In order to introduce a stable numerical scheme, we require the $F \times F$ diagonal diffusivity matrix $\alpha(x) = diag(a_1(x),\ldots,a_F(x))$ to be positive and the forcing term to be uniformly bounded and Lipschitz with respect to its first argument. The following two assumptions are quite natural:

Assumption 3.1 *For all $x \in [0, x_1]$, there exists a constant ξ such that*

$$\min_{1 \le i \le F} a_i(x) \ge \frac{1}{\xi} > 0.$$

Assumption 3.2 *For all $x \in [0, x_1]$, and functions $u, w : [0, x_1] \to \mathbb{R}$ there exist constants L_1 and L_2 such that*

$$\max_{1 \le i \le F} |\, f_i(u,x)| \le L_1$$

and

$$\max_{1 \le i \le F} |\, f_i(u,x) - f_i(w,x)| \le L_2 \,\|u - w\|_\infty .$$

3.1 The Numerical Marching Scheme

Let $\Delta x = h > 0,\ \Delta t = k > 0$. Then for $i = 1,\ldots,M_{\max}$ and $j = 0,\ldots,N_{\max}$, Table 3.1 defines the discrete vector functions that are involved in the numerical marching scheme, as well as the discrete functions that they approximate.

Table 3.1 Vectors and Functions			
$R_i^n \leftrightarrow v(ih, nk)$	$Q_i^n \leftrightarrow a(ih)\, v_x(ih, nk)$	$P_i^n \leftrightarrow v_{xt}(ih, nk)$	$W_i^n \leftrightarrow v_t(ih, nk)$

We begin by performing a mollified differentiation in time of the noisy vector α^ε to determine R_1^n, Q_1^n, P_1^n, and W_1^n. The space marching scheme is defined as follows:

Initialize $i = 1$. Do steps (a) through (f) while $i \le M_{\max} - 1$.

a. $R_{i+1}^n = R_i^n + h\,(diag(a(ih))^{-1} Q_i^n$

b. $Q_{i+1}^n = Q_i^n + h(W_i^n - f(R_i^n, ih))$

c. Choose δ_{i+1}, perform mollified differentiation in time on $J_{\delta_{i+1}}(Q_{i+1}^n)$

d. set $P_{i+1}^n = (diag(a((i+1)h))^{-1} D_{0,t}(J_{\delta_{i+1}}(Q_{i+1}^n))$

e. $W_{i+1}^n = W_i^n + h\, P_i^n$

f. $i = i + 1$.

4. ERROR ESTIMATES

From the numerical scheme, at each marching step, the exact mollified functions v, $a\,v_x$ and v_t can be determined with the local truncation errors evaluated at some intermediate points:

$$new(v) = v + h\, v_x + \frac{h^2}{2} v_{xx},$$

$$new(a\, v_x) = a\, v_x + h\,(v_t - f(v,x)) + \frac{h^2}{2}(a v_x)_{xx},$$

$$new(v_t) = v_t + h\, v_{tx} + \frac{h^2}{2}(v_t)_{xx}.$$

4.1 Stability

In order to determine stability, upper bounds must be found for $\| R_i^n \|_\infty$, $\| Q_i^n \|_\infty$ and $\| W_i^n \|_\infty$ in terms of the initial data.

Theorem 4.1 *If Assumptions 3.1 and 3.2 hold, then there exists a constant* C_1 *such that*

$$\max(\| R_j^n \|_\infty, \| Q_j^n \|_\infty, \| W_j^n \|_\infty) \le \exp(C_1) \max((\| R_0^n \|_\infty, \| Q_0^n \|_\infty, \| W_0^n \|_\infty) + O(h).$$

Proof: At each marching step,

$$\| R_{i+1}^n \|_\infty \le \| R_i^n \|_\infty + \xi\, h \| Q_i^n \|_\infty + O(h^2).$$

Under Assumption 3.2,

$$\| Q_{i+1}^n \|_\infty \le \| Q_i^n \|_\infty + h(\| W_i^n \|_\infty + L_1) + O(h^2).$$

Using Theorem 2.2 and Assumption 3.1,

$$\| W_{i+1}^n \|_\infty \le \| W_i^n \|_\infty + \frac{C \xi h}{\delta} \| Q_i^n \|_\infty + O(h^2).$$

Writing $\bar{C}_1 = \max(1, \xi, \frac{C\xi}{\delta})$,

$$\max(\| R_{i+1}^n \|_\infty, \| Q_{i+1}^n \|_\infty, \| W_{i+1}^n \|_\infty) \le (1 + \bar{C}_1 h) \max(\| R_i^n \|_\infty, \| Q_i^n \|_\infty, \| W_i^n \|_\infty) + O(h),$$

and, after j iterations,

$$\max(\| R_j^n \|_\infty, \| Q_j^n \|_\infty, \| W_j^n \|_\infty) \le (1 + \bar{C}_1 h)^j \max(\| R_0^n \|_\infty, \| Q_0^n \|_\infty, \| W_0^n \|_\infty) + O(h).$$

The thesis follows immediately from the last expression.

4.2 Error Analysis

Let $\Delta_i = \max(\| \Delta R_i^n \|_\infty, \| \Delta Q_i^n \|_\infty, \| \Delta W_i^n \|_\infty)$, where $\Delta R_i^n = R_i^n - v(ih, nk)$, $\Delta Q_i^n = Q_i^n - a(ih)\, v_x(ih, nk)$, and $\Delta W_i^n = W_i^n - v_t(ih, nk)$. The following theorem states that the marching scheme is convergent.

Theorem 4.2 Under *Assumptions 3.1, 3.2, there exists a constant* C_2 *such that*

$$\Delta_j \le \exp(C_2) \Delta_0 + O(h^2) + O(k).$$

Proof: From Assumptions 3.1 and 3.2,

$$\| \Delta R_{i+1}^n \|_\infty \le \| \Delta R_i^n \|_\infty + \xi\, h \| \Delta Q_i^n \|_\infty + O(h^2)$$

and

$$\| \Delta Q_{i+1}^n \|_\infty \le \| \Delta Q_i^n \|_\infty + h(\| \Delta W_i^n \|_\infty + L_2 \| \Delta R_i^n \|_\infty) + O(h^2).$$

Using Lemma 2.1,

$$\| \Delta W_{i+1}^n \|_\infty \le \| W_i^n \|_\infty + \frac{C \xi h}{\delta}(\| \Delta Q_i^n \|_\infty + k) + C_\delta k^2 + O(h^2),$$

where C_δ is an upper bound, in magnitude, of higher order derivatives of ρ_δ.

Define $\bar{C}_2 = \max(1 + L_2, \xi, \frac{C\xi}{\delta})$. Then

$$\Delta_{i+1} \le (1 + \bar{C}_2 h) \Delta_i + O(h^2) + O(k)$$

and, after j iterations,

$$\Delta_j \le (1+\bar{C}_2 h)^j \Delta_0 + O(h^2) + O(k) \le \exp(1+\bar{C}_2\, j\, h)\Delta_0 + O(h^2) + O(k)\,.$$

Notice that $\Delta_0 \le \dfrac{C}{\delta}(\varepsilon + h)$. Thus, for fixed δ, as ε, h, and k tend to 0 then so does Δ_j.

Therefore, the numerical marching scheme presented in section 3 is formally convergent.

5. NUMERICAL EXAMPLES

In this section, we present two examples of interest. In each of these examples, the parameter *p*, introduced in section 2, has been set to 3. The radii of mollification have been chosen automatically using the GCV method.

In each of the examples we begin by solving the corresponding direct problem in order to obtain the boundary data for the inverse problem. In what follows, when compared to the reconstructed solution, "exact solution" means numerical solution of the direct problem.

Discretized measured approximations of the Cauchy data are modeled by adding random errors to the "exact solution" sampled data. The errors of all the recovered functions are measured by relative weighted l^2 - norms defined by

$$\left[\frac{1}{(M_{\max}+1)(N_{\max}+1)}\sum_{i=0}^{M_{max}}\sum_{n=0}^{N_{\max}} | v(ih,nk) - R_i^n |^2\right]^{1/2} / \left[\frac{1}{(M_{\max}+1)(N_{\max}+1)}\sum_{i=0}^{M_{\max}}\sum_{n=0}^{N_{\max}} | v(ih,nk) |^2\right]^{1/2}.$$

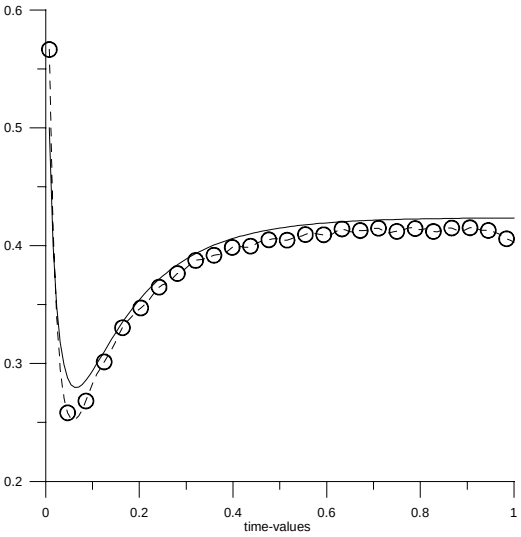

Figure 5.1.1 Example 5.1. Exact and computed solutions for $u_1(0.5,t)$.

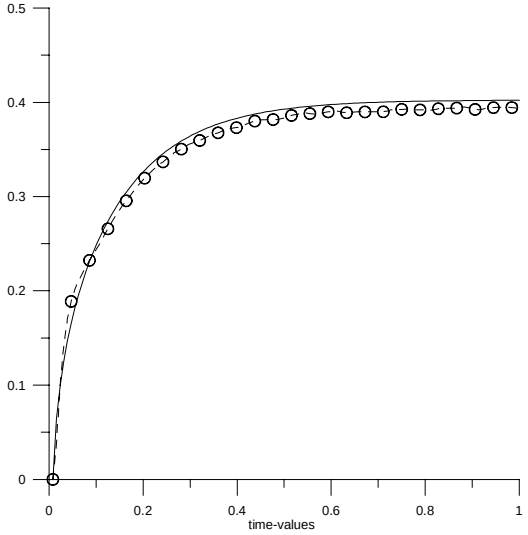

Figure 5.1.2 Example 5.1. Exact and computed solutions for $u_2(0.5,t)$.

Example 5.1 – Chemical Reaction

Identify $u_1(x,t)$, $u_2(x,t)$, $u_1(x,0)$ and $u_2(x,0)$ satisfying

$$\begin{aligned}
&(u_1)_t = (u_1)_{xx} - e^{6(u_1-u_2)} + e^{-11(u_1-u_2)},\\
&(u_2)_t = (u_2)_{xx} + e^{5(u_1-u_2)} - e^{-11(u_1-u_2)},\\
&0 < x < 0.5,\ 0 < t < 1,\\
&u_1(0,t) = 0,\\
&u_2(0,t) = 0,\\
&(u_1)_x(0,t) = \alpha_1(t),\\
&(u_2)_x(0,t) = \alpha_2(t),\\
&0 \le t \le 1.
\end{aligned}$$

Discretized versions of $\alpha_1(t)$ and $\alpha_2(t)$ are determined by solving the direct initial value problem with

$$u_1(x,0) = x,\ u_2(x,0) = 0,\ u_1(1,t) = 1 \text{ and } (u_2)_x(1,t) = 0.$$

Table 5.1 shows the discrete relative l^2 errors of the solutions and the gradient components as functions of the amount of noise in the data, ε. For this table as well as for the figures, $\Delta t = 1/128$ and $\Delta x = 1/100$. All the pictures correspond to maximum noise level $\varepsilon = 0.005$.

Figures 5.1.1-5.1.9 illustrate the excellent agreement between the exact and computed solutions, exact and computed initial conditions, and exact and computed gradient function components for example 5.1. Note the different scales used in the pictures.

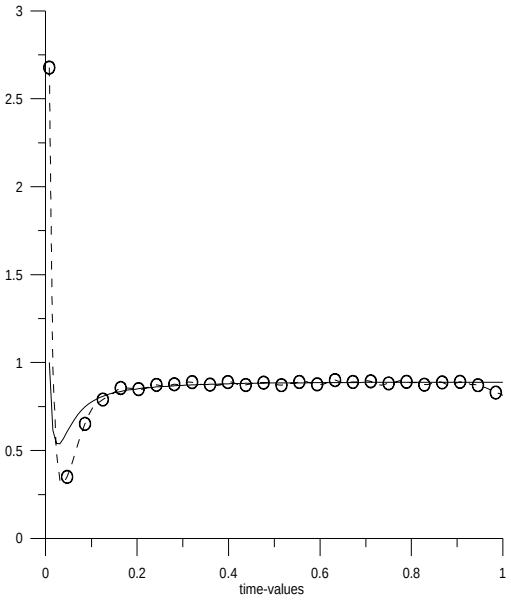

Figure 5.1.3 Example 5.1. Exact and computed solutions for $(u_1)_x(0.5,t)$.

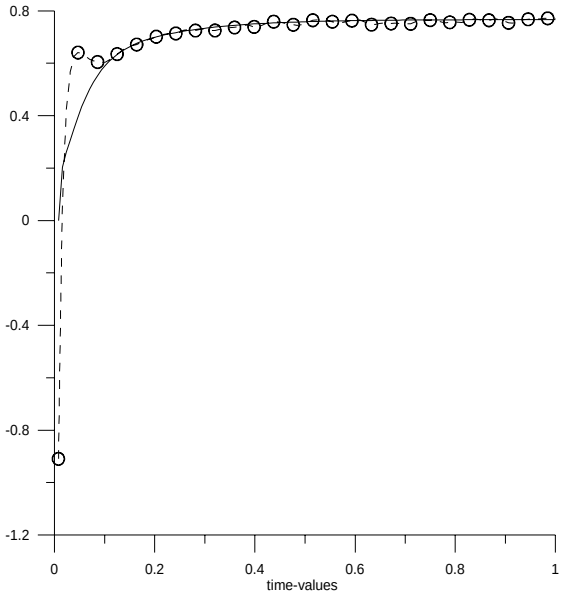

Figure 5.1.4 Example 5.1. Exact and computed solutions for $(u_2)_x(0.5,t)$.

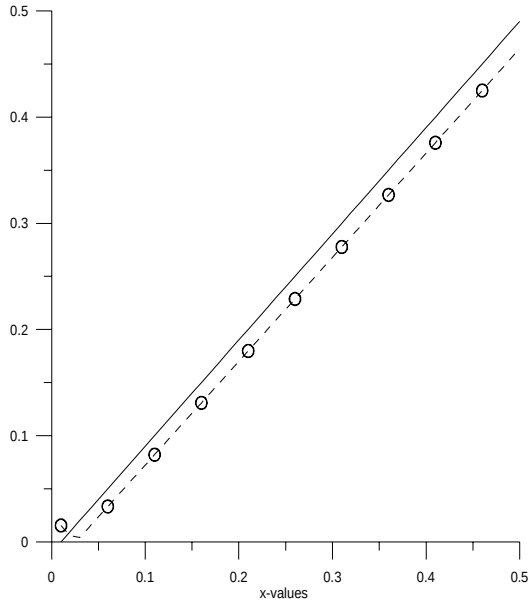

Figure 5.1.5 Example 5.1. Exact and computed solutions for $u_1(x,0)$.

ε	0.0010	0.0050	0.0100
u_1	0.0099	0.0104	0.0112
u_2	0.0123	0.0122	0.0122
$(u_1)_x$	0.0519	0.0521	0.0568
$(u_2)_x$	0.0410	0.0407	0.0459
$(u_1)_t$	0.0130	0.0129	0.0155
$(u_2)_t$	0.0321	0.0322	0.0348

Table 5.1 Example 5.1. Relative l^2 errors in $[0,0.5]\times[0,1]$.

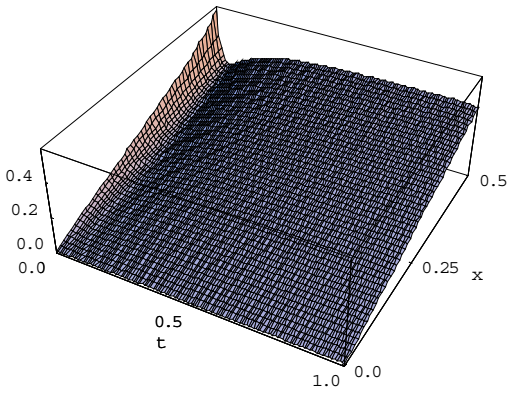

Figure 5.1.6 Example 5.1. Exact $u_1(x,t)$.

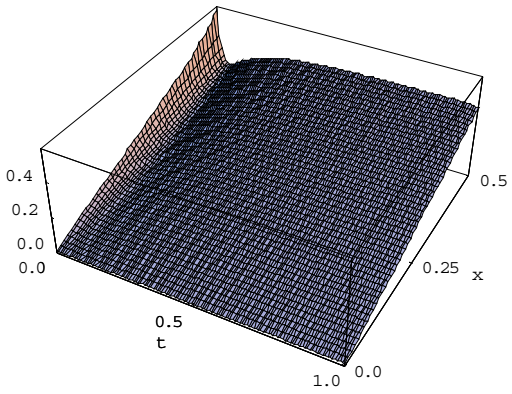

Figure 5.1.7 Example 5.1.Computed $u_1(x,t)$.

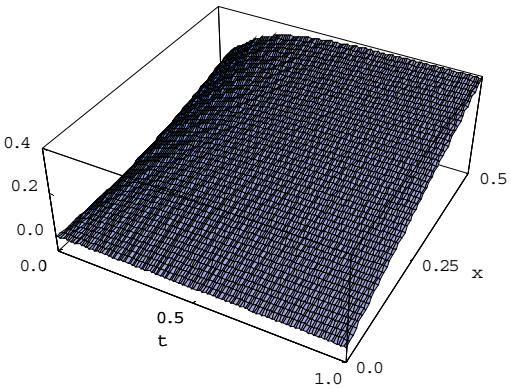

Figure 5.1.8 Example 5.1.Exact $u_2(x,t)$.

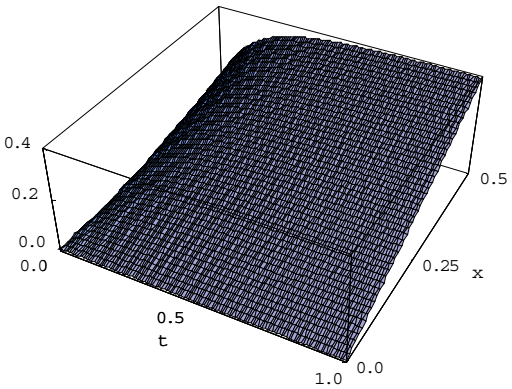

Figure 5.1.9 Example 5.1.Computed $u_2(x,t)$.

Example 5.2 - Lotka-Volterra System

We restrict our attention to models where the coefficients, the initial and the boundary conditions are chosen such that the solution functions are positive and reach quasy-steady state (numerical equilibrium) in a finite time.

As in the previous example, we wish to identify $u_1(x,t)$, $u_2(x,t)$, $u_1(x,0)$ and $u_2(x,0)$ satisfying

$$
\begin{aligned}
&(u_1)_t = (u_1)_{xx} + u_1(b_1(x) + c_1(x)u_1 + d_1(x)u_2),\\
&(u_2)_t = (u_2)_{xx} + u_2(b_2(x) + c_2(x)u_2 + d_2(x)u_1),\\
&0 < x < 0.5,\ 0 < t < 1,\\
&(0,t) = 0,\\
&u_2(0,t) = 0,\\
&(u_1)_x(0,t) = \alpha_1(t),\\
&(u_2)_x(0,t) = \alpha_2(t),\\
&0 \le t \le 1,
\end{aligned}
$$

with

$$
\begin{aligned}
&b_1(x) = 5,\\
&b_2(x) = 3,\\
&c_1(x) = -10,\\
&c_2(x) = -2x^2,\\
&d_1(x) = -2x,\\
&d_2(x) = -3.
\end{aligned}
$$

Discretized versions of $\alpha_1(t)$ and $\alpha_2(t)$ are determined by solving the direct initial value problem with

$$u_1(x,0)=\sin(x),\ u_1(\pi,t)=0,\ u_2(x,0)=-2x(\pi-x) \text{ and } u_2(\pi,t)=0.$$

Coexistence of these two species becomes possible only if $|\frac{c_1}{b_1}>\frac{c_2}{b_2}|$ and $|\frac{d_2}{b_2}>\frac{d_1}{b_1}|$, [1], [4], [5].

Table 5.2 shows the discrete relative l^2 errors of the solutions and the gradient components as functions of the amount of noise in the data, ε. For this table as well as for the figures, $\Delta t=1/128$ and $\Delta x=1/100$. All the pictures correspond to the maximum level of noise $\varepsilon=0.005$.

ε	0.0010	0.0050	0.0100
u_1	0.0095	0.0095	0.0123
u_2	0.0195	0.0196	0.0202
$(u_1)_x$	0.0173	0.0174	0.0122
$(u_2)_x$	0.0353	0.0353	0.0352
$(u_1)_t$	0.0125	0.0125	0.0179
$(u_2)_t$	0.0226	0.0226	0.0230

Table 5.2 Example 5.2 Relative l^2 errors in $[0,0.5]\times[0,1]$

Figures 5.2.1-5.2.5 show the good agreement between the exact and computed solutions, exact and computed initial conditions, and exact and computed gradient function components for example 5.2. Note the different scales used in the pictures.

5.1 <u>Identification of Coefficients</u>

If the initial conditions are approximately known in Example 5.2, we examine the related new inverse problem:

Example 5.2.a - Recovering Coefficients

Identify $u_1(x,t)$, $u_2(x,t)$, $b_1(x)$ and $b_2(x)$ satisfying

$$\frac{\partial u_1}{\partial t}=\frac{\partial^2 u_1}{\partial x^2}+u_1(b_1(x)+c_1(x)u_1+d_1(x)u_2),$$
$$\frac{\partial u_2}{\partial t}=\frac{\partial^2 u_2}{\partial x^2}+u_2(b_2(x)+c_2(x)u_2+d_2(x)u_1),$$
$$u_1(x,0)\approx\sin(x),\ u_2(x,0)\approx-2x(\pi-x),$$
$$0<x<0.5,\ 0<t<1,$$
$$u_1(0,t)=0,$$
$$u_2(0,t)=0,$$
$$(u_1)_x(0,t)=\alpha_1(t),$$
$$(u_2)_x(0,t)=\alpha_2(t),$$
$$0\le t\le 1.$$

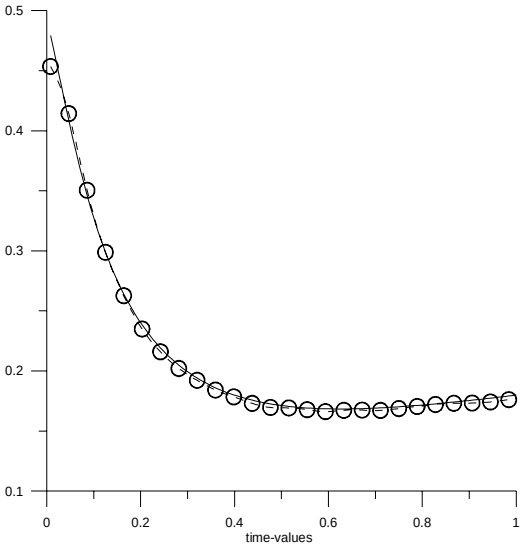

Figure 5.2.1 Example 5.2. Exact and computed solutions for $u_1(0.5,t)$.

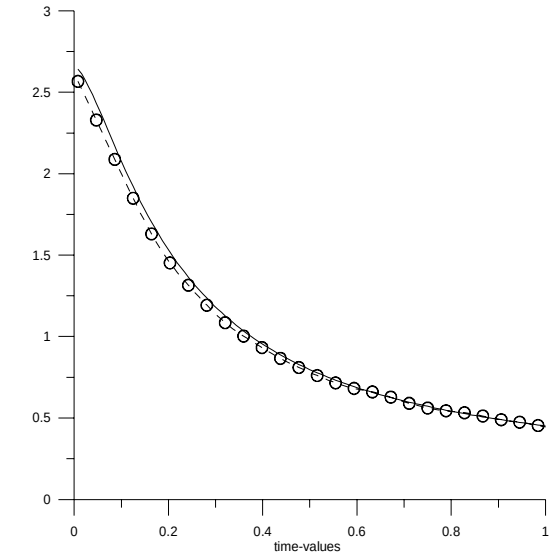

Figure 5.2.2 Example 5.2. Exact and computed solutions for $u_2(0.5,t)$.

Assuming exact measurements at $t=0$, the formulae for $b_1(x)$, (similarly for $b_2(x)$), is given by

$$b_1(x)=[\frac{\partial u_1}{\partial t}-\frac{\partial^2 u_1}{\partial x^2}-c_1(x)(u_1)^2-d_1(x)u_1u_2]/u_1.$$

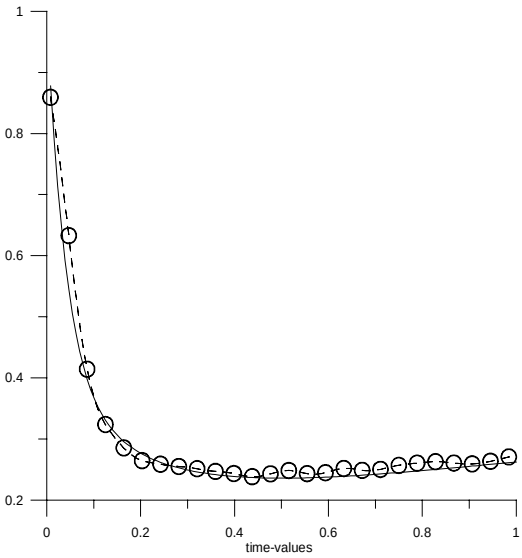

Figure 5.2.3 Example 5.2. Exact and computed solutions for $(u_1)_x(0.5,t)$.

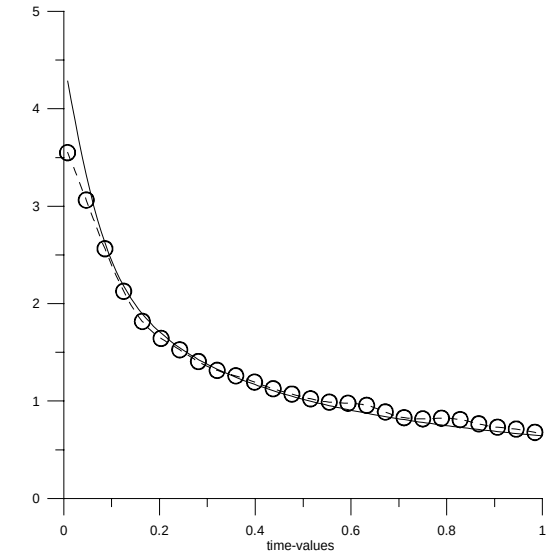

Figure 5.2.4 Example 5.2. Exact and computed solutions for $(u_2)_x(0.5,t)$.

Note that it is possible to recover any pair of unknown coefficients (one in each partial differential equation).

For noisy data, this expression is useless since it requires the evaluation of two partial derivatives from inexact data. Moreover, it can only be used at points where u_1 is different from zero. This implies that the numerical reconstruction of the coefficients is not possible near the active boundary and we have to restrict the solution of the inverse problem for the coefficients to a suitable compact subset of the original domain.

The set of admissible points, $\Gamma_\delta^\varepsilon$, where the mollified or regularized formula for the coefficients can be applied, is defined as the set of grid points $(x_i,0),\ 0<x_i<0.5,$ for which $(u_1)_\delta^\varepsilon(x_i,0)>3\delta>0$. The set $\Gamma_\delta^\varepsilon$ can be completely determined before starting the marching procedure or it can be dynamically built during the marching scheme. The mollified or regularized formula for the approximate identification of $b_1(x)$ is

$$(b_1)_\delta^\varepsilon(x)=[\frac{\partial (u_1)_\delta^\varepsilon}{\partial t}-\frac{\partial^2 (u_1)_\delta^\varepsilon}{\partial x^2}-c_1(x)((u_1)_\delta^\varepsilon)^2-d_1(x)(u_1)_\delta^\varepsilon(u_2)_\delta^\varepsilon]/(u_1)_\delta^\varepsilon$$

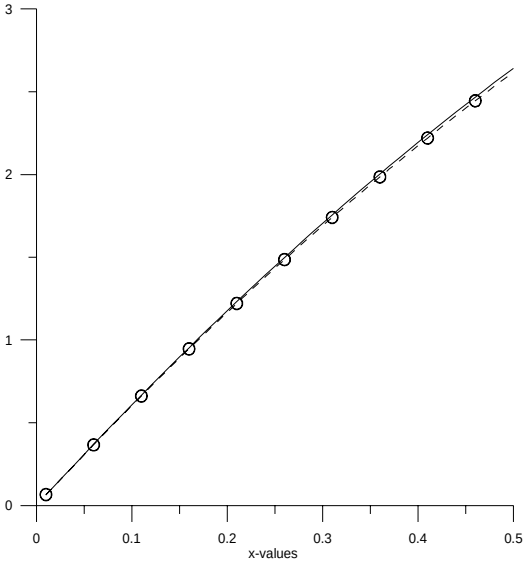

Figure 5.2.5 Example 5.2. Exact and computed solutions for $u_2(x,0)$.

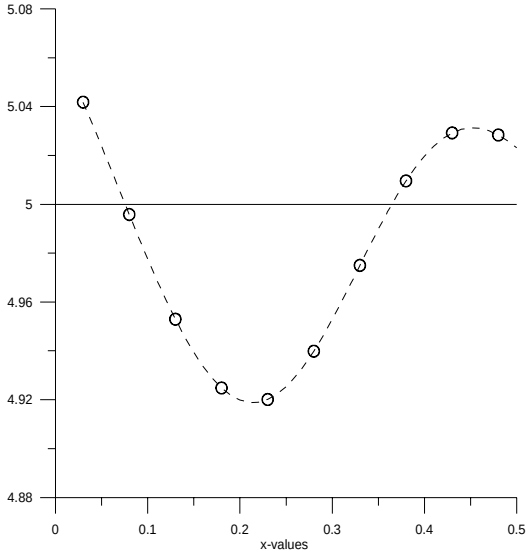

Figure 5.2.6 Example 5.2. Exact and computed coefficients for $b_1(x)$.

where the temporal partial derivatives are obtained, at each step in space, from the marching algorithm. An estimate of the error term $\| b_1 - (b_1)_\delta^\varepsilon \|_{\infty,\Gamma_\delta^\varepsilon}$ will be provided elsewhere.

Figure 5.2.6 shows the qualitative behavior of the reconstructed coefficient $b_1(x) = 5$ on the interval $(0, 0.5)$ with $\Gamma_\delta^\varepsilon \subseteq [0.03, 0.5]$.

6. CONCLUSIONS

The approach and results offered in this presentation indicate that the methodology is very useful to approximately recover solutions, initial conditions and gradient components of nonlinear systems of partial differential equations, from Cauchy data given at the active boundary of the domain. If the initial conditions of the original direct problem are known, it is also possible to identify suitable space dependent coefficients in Lotka-Volterra biological systems with diffusion. An extension of the procedures to higher dimensional cases is straightforward.

Acknowledgment

This work was partially supported by a C. Taft fellowship.

REFERENCES

1. A.W. Leung, *Systems of Nonlinear Partial Differential Equations: Applications to Biology and Engineering*, Kluwer, Dordrecht-Boston, 1989.

2. D.A. Murio, Mollification and Space Marching, chapter **4**, *Inverse Engineering Handbook*, (ed. K. Woodbury), CRC Press, Boca Raton, Florida, 2002, pp. 219-326.

3. D.A. Murio, C.E. Mejía and S. Zhan, Discrete Mollification and Automatic Numerical Differentiation, *Computers Math. Applic.* (1998) **35**(5), 1-16.

4. C.V. Pao, *Nonlinear Parabolic and Elliptic Equations*, Plenum Press, New York, 1992.

5. A. Okubo, A. and S. Levin, *Diffusion and Ecological Problems: Modern Perspectives*, 2nd ed. Springer-Verlag, New York, NY, 2001.

6. G. Wahba, *Spline Models for Observational Data*, CBMS-NSF Regional Conferences Series in Applied Mathematics, SIAM, Philadelphia, 1990.